World Academy of Science, Engineering and Technology
International Journal of Mechanical and Mechatronics Engineering
Vol:3, No:9, 2009

Numerical Simulations of Cross-Flow around Four Square Cylinders in an In-Line Rectangular Configuration

Shams Ul Islam, Chao Ying Zhou, and Farooq Ahmad

***Abstract*—**A two-dimensional numerical simulation of cross-flow around four cylinders in an in-line rectangular configuration is studied by using the lattice Boltzmann method (LBM). Special attention is paid to the effect of the spacing between the cylinders. The Reynolds number (R_e) is chosen to be $R_e = 100$ and the spacing ratio L/D is set at 0.5, 1.5, 2.5, 4.0, 5.0, 6.0, 7.0, 8.0, 9.0 and 10.0. Results show that, as in the case of four cylinders in an in-line rectangular configuration , flow fields show four different features depending on the spacing (single square cylinder, stable shielding flow, wiggling shielding flow and a vortex shedding flow) are observed in this study. The effects of spacing ratio on physical quantities such as mean drag coefficient, Strouhal number and root-mean-square value of the drag and lift coefficients are also presented. There is more than one shedding frequency at small spacing ratios. The mean drag coefficients for downstream cylinders are less than that of the single cylinder for all spacing ratios. The present results using the LBM are compared with some existing experimental data and numerical studies. The comparison shows that the LBM can capture the characteristics of the bluff body flow reasonably well and is a good tool for bluff body flow studies.

***Keywords*—**Four square cylinders, Lattice Boltzmann method, rectangular configuration, spacing ratios, vortex shedding.

I. Introduction

FLOW around a group of cylinders is of practical importance in many fields of engineering, such as flow around cables, heat exchanger tube arrays, etc. The effects of the flow interference among the cylinders strongly depend on the arrangement of the cylinders. The interference effects strongly depend on the arrangement of the two cylinders Zdravkovich [1]. He categorized the two cylinders arrangements into three types: side-by-side, tandem and staggered arrangements. Sayers [2] experimentally measured the lift and drag coefficient on a single cylinder in a group of four equally spaced cylinders in an open-jet wind tunnel at spacing ratios ranging from 1.1 to 5.0 and Reynolds number ($R_e = 3.0\times10^4$). Later, Sayers [3] further measured the Strouhal number (S_t) of each cylinder in the same open-jet wind tunnel. Lam and Luo [4] had conducted a visualization study at spacing ratios ranging from 1.28 to 5.96 and $R_e = 2.1\times10^3$ and summarized the flow characteristics into three different flow patterns. Lam and Fang [5] experimentally determined the effects of flow interference of four cylinder array at spacing ratios ranging from 1.26 to 5.80 and $R_e = 12.8\times10^3$. Zdravkovich [6] and Norberg [7] numerically investigated the flow around single and multiple cylinders cover a wide range of Reynolds numbers, from 40 to 2.0×10^6. However, numerical studies of the flow around four cylinders in an in-line square configuration are relatively few. Farrant *et* al [8] and Lam *et al* [9] numerically studied the flow around four cylinders using a cell boundary element method and surface vorticity method, at $R_e = 200$ by Farrant *et* al. in [8] and at $R_e = 1.3\times10^3$ by Lam *et al* [9], respectively. They observed different flow patterns such as in-phase vortex shedding, anti-phase vortex shedding and synchronized mode. Lam *et al* [10] further numerically observed some interesting observations. Further Lam *et al* [11] carried out two- and three-dimensional numerical simulations of cross-flow around four cylinders in an in-line square configuration using a finite-volume method at spacing ratios ranging from 1.6 to 5.0 at Reynolds numbers 100 and 200. They observed three distinct flow patterns for two-dimensional studies: (i) a stable shielding flow; (ii) a wiggling shielding flow and (iii) a vortex shedding flow.

On the other hand, there have been numerous detailed studies of flow past a square cylinder in two-dimensions as well as three-dimensions for side-by-side, tandem, staggered and single square cylinders. Inoue *et al* [12] numerically investigated flow around two square cylinders for side-by-side arrangement. They paid special attention to the effect of the spacing between the two cylinders at $R_e = 150$. They observed six different flow patterns: anti-phase and in-phase synchronized, flip-flopping, single bluff-body and steady patterns. Recently, the flow around side-by-side square cylinders numerically investigated by Rao *et al* [13] using the lattice Boltzmann method. They examined the flip-flop regime at small space ratios and the synchronized regime at large space ratios. Degawa and Uchiyama [14] numerically

Shams Ul Islam is with the Mechanical Engineering and Automation Department, Harbin Institute of Technology, Shenzhen Graduate School, Shenzhen 518055, China (corresponding author, Phone: 0086-15016705177; Fax: 0086-755-26033774; e-mail: shams804@hotmail.com).

Chao Ying Zhou is with the Mechanical Engineering and Automation Department, Harbin Institute of Technology, Shenzhen Graduate School, Shenzhen 518055, China (e-mail: cyzhou@hit.edu.cn).

Farooq Ahmad is with the Computer science Department, Harbin Institute of Technology Shenzhen Graduate School, China (e-mail: farooq190@gmail.com).

examined bubbly flow around two tandem square cylinders using vortex method. They observed that the strength of the Karman vortex downstream of the second cylinder is larger than that for the single-cylinder at Reynolds number 10000. A number of studies have been done so far, especially on the flow around a single square and rectangular cylinder [15-18].

As mentioned above there have been some experimental and numerical studies for different flow configurations, however, the investigations of the spacing effects on the flow characteristics for four square cylinders in an in-line rectangular configuration has far from completed especially at low Reynolds number for laminar flows. The quantitative information of the changes in vortex structures, the changes in physical quantities and the variations in force coefficients is quite far from completed. Regarding the available studies in the literature, the present study provides further computational information and close investigation on the spacing effect of a four square cylinders in an in-line rectangular configuration at low Reynolds number. The effects of the spacing on the force coefficients, the Strouhal number and the flow structures in the near wake are reported in detail. The LBM with the incompressible Bhatnagar-Gross-Krook (LBGK) model are used for the fluid flow simulation and the results are compared with related data published in the literature for single square cylinder especially experimentally.

The rest of this paper is organized as follows. A brief description of the problem to be considered is given in Section II and a detailed description of the lattice Boltzmann method (LBM) together with the boundary is presented in Section III. The results on the effects of the spacing on the force coefficients, vortex shedding frequency and the flow structures are discussed in Section IV. Finally conclusions are drawn in Section V.

II. Problem Description

The schematic configuration of a rectangular cylinder in a uniform flow is shown in Fig.1 where D is the diameter of the cylinder and L is the centre-to-centre spacing between cylinders, and U_∞ is the velocity of the uniform flow. A computational domain with $10D$ upstream, $40D$ downstream and a distance of $12.5D$ on either sides of the cylinder in transverse direction is selected for the present simulations, which has been proved to provide a good compromise between accuracy of the solution and computational cost for a uniform flow past a cylinder [19].

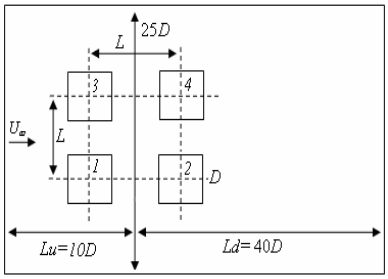

Fig. 1 Arrangement and computational domain for a four-cylinder array

III. Numerical Method

Instead of solving the usual continuum equations for the conserved fluid fields, the lattice Boltzmann method (LBM) models the fluid flow by tracking the evolution of fluid particles where the physical space are discretized into a number of square regular lattices and at each time step the particles move and collide following certain rules. In the present study, a two-dimensional nine-velocity (D2Q9) model and the Bhatnagar-Gross-Krook (BGK) collision model used in the standard Boltzmann equation are adopted [20].

The evolution equation of the density distribution function of the fluid particles can be described by

$$g_i\left(\boldsymbol{x}+c\boldsymbol{e}_i\Delta t, t+\Delta t\right)-g_i\left(\boldsymbol{x},t\right)=\Omega_i(g) \tag{1}$$

where $g_i(\boldsymbol{x},t)$ is the density distribution function of the particle at position $\boldsymbol{x}$ and time t with velocity $c\boldsymbol{e}_i$, Δx and Δt are the lattice grid spacing and the time step, $c=\Delta x/\Delta t$ is the particle speed and $\boldsymbol{e}_i$ is the direction of the velocity, and Ω_i is the collision operator which must maintain the total mass and momentum of the particle system. The fluid density ρ is then obtained from the density distribution function by

$$\rho=\sum_i g_i \tag{2}$$

The density distribution function $g_i(x,t)$ is modified at each time step according to the evolution of the particles.

In the two-dimensional nine-velocity (D2Q9) model, each lattice node has eight nearest neighbors connected by eight links and the particles move only along the axes or the diagonal directions of the lattices (see Fig. 2). The directions of the discrete velocity are given by

$$\boldsymbol{e}_i=\begin{cases}(0,0) & i=0\\ \left(\cos\left|(i-1)\pi/2\right|,\sin\left|(i-1)\pi/2\right|\right) & i=1,2,3,4\\ \sqrt{2}\left(\cos\left|(i-5)\pi/2+\pi/4\right|,\sin\left|(i-5)\pi/2+\pi/4\right|\right) & i=5,6,7,8\end{cases} \tag{3}$$

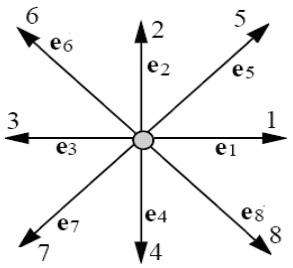

Fig. 2 Two-dimensional nine-velocity lattice (D2Q9) model

Bhatnagar, Gross and Krook (BGK) [21] described a collision operator to consider the collision effects between particles where the collision process was described as a relaxation process to the local equilibrium state in the following way:

$$\Omega_i=-\frac{1}{\tau}\left[g_i\left(\boldsymbol{x},t\right)-g_i^{(0)}\left(\boldsymbol{x},t\right)\right] \tag{4}$$

where τ is the non-dimensional relaxation and $g_i^{(0)}\left(\boldsymbol{x},t\right)$ is an equilibrium distribution function. The equilibrium distribution chosen from [20] is defined by

$$g_i^{(0)}(\boldsymbol{x},t)=\alpha_i p+\omega_i\left[3\frac{(\boldsymbol{e_i}\cdot\boldsymbol{u})}{c}+4.5\frac{(\boldsymbol{e_i}\cdot\boldsymbol{u})^2}{c^2}-1.5\frac{|\boldsymbol{u}|^2}{c^2}\right]. \quad (5)$$

Where

$$\alpha_i=\begin{cases}-4\dfrac{\sigma}{c^2} & i=0\\ \dfrac{\lambda}{c^2} & i=1,2,3,4\\ \dfrac{\gamma}{c^2} & i=5,6,7,8\end{cases} \quad \text{and} \quad \omega_i=\begin{cases}\dfrac{4}{9} & i=0\\ \dfrac{1}{9} & i=1,2,3,4\\ \dfrac{1}{36} & i=5,6,7,8\end{cases} \quad (6)$$

and σ, λ, γ are parameters satisfying λ + γ = σ and λ + 2γ = 1/2.

The evolution equation of the density distribution function is then described by the following single-relaxation-time BGK equation

$$g_i\left(\boldsymbol{x}+c\boldsymbol{e}_i\Delta t,t+\Delta t\right)=g_i\left(\boldsymbol{x},t\right)-\frac{1}{\tau}\left[g_i\left(\boldsymbol{x},t\right)-g_i^{(0)}\left(\boldsymbol{x},t\right)\right] \quad (7)$$

(*i=0,1,2,…,8*)

The incompressible Navier–Stokes equations can be recovered from incompressible LBGK models [20, 22].

The kinematic viscosity ν can be obtained in the following way

$$\nu=c_s^2\left(\tau-\frac{1}{2}\right)\frac{\Delta x^2}{\Delta t} \quad (8)$$

where $c_S=\frac{c}{\sqrt{3}}$ is the speed of sound. A careful selection of τ is very important in lattice Boltzmann (LB) modeling since the numerical stability and computational cost depend on the value of τ. The flow velocity and pressure can be obtained by

$$\boldsymbol{u}=\sum_{i=1}^{8}c\boldsymbol{e}_i g_i \quad (9)$$

$$p=\frac{c^2}{4\sigma}\left[\sum_{i=1}^{8}g_i-\frac{2|\boldsymbol{u}|^2}{3c^2}\right] \quad (10)$$

More details can be found in [20].

Inlet boundary: Uniform flow with velocity U_∞ is incorporated in using the equilibrium particle distribution function (PDF) at the inlet boundary where

$$u=U_\infty \text{ and } v=0 \quad (11)$$

Outlet boundary: The computational domain behind the cylinder is selected to be large enough so that the flow at the outflow boundary can be considered to be fully developed. Therefore a zeroth order approximation for PDF is adopted at the outlet boundary.

Surface of the cylinder: No-slip wall boundary condition is applied to the surface, which is;

$$u=0 \text{ and } v=0. \quad (12)$$

This is realized using a bounce-back treatment in which all particles hitting the solid wall and reflected back to its previous position.

Top and bottom boundaries: Uniform flow boundary condition is applied at both top and bottom boundaries of the computational domain.

$$u=U_\infty \text{ and } v=0 \quad (13)$$

The total fluid force F on the square cylinder is calculated using the momentum exchange method [23]. The force is given by;

$$F=\sum_{all\ x_b}\sum_{\alpha=1}^{N}e_\beta\left[n_\alpha\left(x_b,\ t\right)+n_\alpha\left(x_b+e_\beta\Delta t,\ t\right)\right]\frac{\Delta x}{\Delta t}. \quad (14)$$

Where N is the number of non-zero lattice velocity vectors, the subscript α is the opposite lattice direction of β, i.e. $\alpha=\beta=1,2,\ldots,8$. To obtain the fluid solid momentum exchange per unit time equation (14) is treated at the midpoint for the fluid lattice node $x_f=\left(x_b+ce_\beta\Delta t,\ t\right)$ and the solid lattice node $x_b=\left(x_f+ce_a\Delta t,\ t\right)$, where x_b denotes the solid nodes and x_f represents the fluid nodes. The momentum exchange between a solid node at x_b and all possible neighboring fluid nodes around that solid node can be obtained by the inner summation, while the force contribution for all boundary nodes at x_b is given by the outer summation.

Reynolds number *Re* is defined by

$$R_e=\frac{U_\infty D}{\nu} \quad (15)$$

Other important parameters are the Strouhal number S_t, the drag coefficient C_d, and the lift coefficient C_l. They are defined by the following formulas

$$S_t=\frac{f_s D}{U_\infty} \quad (16)$$

$$C_d=\frac{F_d}{\frac{1}{2}\rho U_\infty^2 D} \quad (17)$$

$$C_l=\frac{F_l}{\frac{1}{2}\rho U_\infty^2 D} \quad (18)$$

where f_s is the vortex shedding frequency from the cylinder, F_d and F_l are the force components in the in-line and transverse directions, respectively.

Computations are normally terminated when the following convergence criteria is satisfied

$$\frac{\sqrt{\sum_{l,m}\left[u_{l,m}^{(k+1)}-u_{l,m}^{(k)}\right]^2}}{\sqrt{\sum_{l,m}\left[u_{l,m}^{(k+1)}\right]^2}}\le 1\times10^{-6} \quad (19)$$

All the computations are carried out on a Dawning Parallel Computer TC4000.

IV. Results and Discussion

In order to investigate the effects of the spacing ratio, ten values of L/D between 0.5 and 10 are selected. The drag and lift coefficients, the vortex shedding frequency and the flow structure are analyzed for the purpose. The numerical scheme as explained above is validated for the case of single square cylinder. Results are compared in Table I. Moreover, Table I shows the computed mean drag coefficient and Strouhal number. For the uniform approach flow, computed results are compared with some available experimental and numerical data from open literature and found to be in good agreement.

TABLE I
COMPARISON OF SINGLE SQUARE CYLINDER: STROUHAL NUMBER AND MEAN COEFFICIENT OF DRAG RESULTS WITH SIMULATIONS AND EXPERIMENTS AT $R_e = 100$

Author	Mean Drag Coefficient	Strouhal number
Shimizu and Tanida [15] exp	1.5	--
Okajima [16] exp	--	0.141-0.145
Norberg [17] exp	--	0.143
Sohankar *et al.* [18] num	1.44	0.145
Present	1.3359	0.1472

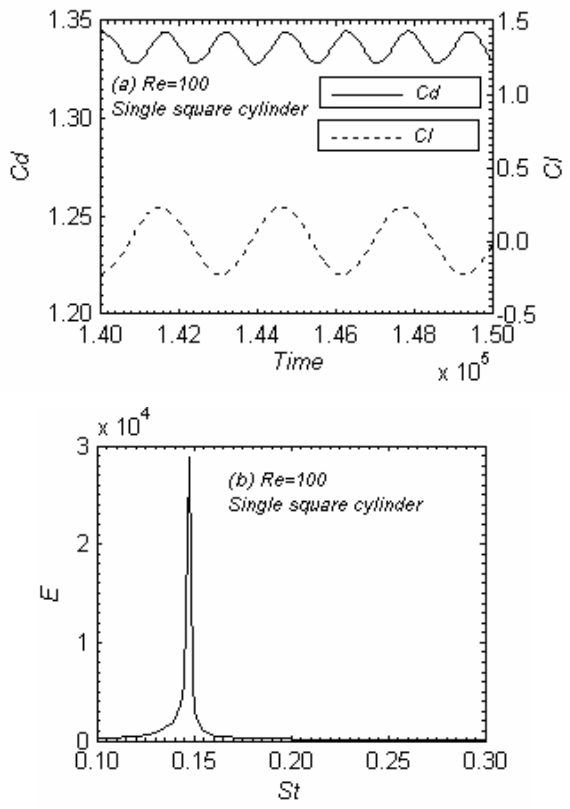

Fig. 3 (a) Variation of lift and drag coefficient for single square cylinder and (b) Fourier spectrum analysis of lift coefficient for single square cylinder

In Fig. 3(a) shows the solid line represents the drag coefficient and the dotted line indicates the lift coefficient. It is seen that the periodic vortex shedding behavior is well captured by the LBM method. The frequency of the drag coefficient is twice that of the lift coefficient. Fig. 3(b) shows the spectra of the time-varying lift coefficient obtained by fast Fourier transform. The frequency value read directly from the spectra give the Strouhal number.

A. Drag and lift force coefficients

For the sake of brevity, only two groups of force time histories are presented. The first one is illustrated in Fig. 4 where L/D is kept at 1.5. The second one is plotted in Fig. 5 where L/D is kept at 10.0. The solid line represents the drag coefficient and the dotted line indicates the lift coefficient. The results show that the vortex shedding becomes irregular, and the frequencies of the lift and drag coefficients are not periodic for small spacing ratio (see Fig. 4). On the other hand, the frequency of the lift coefficient is twice that of the drag coefficient for all cylinders for higher spacing ratios such as 10.0 (see Fig. 5). However, at spacing ratio 10.0, for the drag coefficient for all four cylinders in figure 5, it is not a simple sine wave and there seems to be a small modulation in shedding frequency for the downstream cylinders 2 and 4 and much more modulations for upstream cylinders 1 and 3 as compared to downstream cylinders. Such modulation is not happened for single square cylinder (see Fig. 3(a)). The reason is may be there are upstream cylinders in the wake of downstream cylinders.

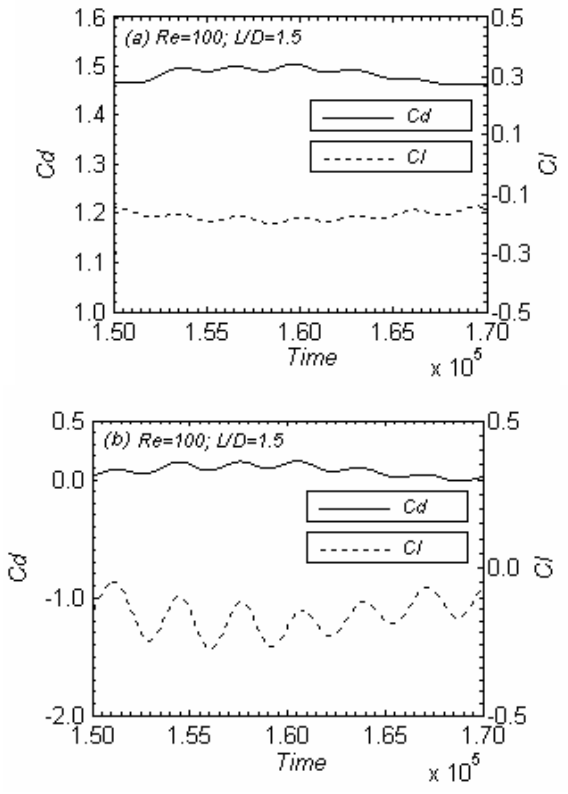

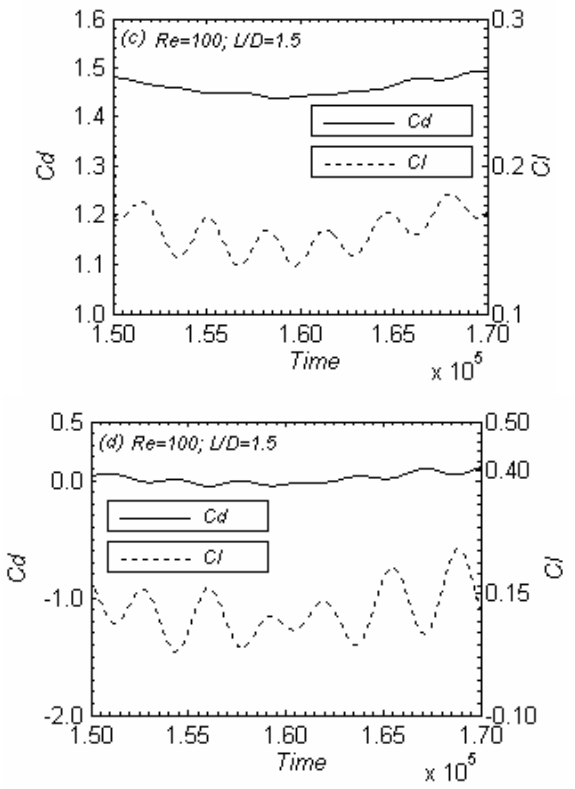

Fig. 4 Variation of lift and drag coefficient for spacing ratio 1.5 (a) Cylinder1, (b) Cylinder2, (c) Cylinder3, (d) Cylinder4

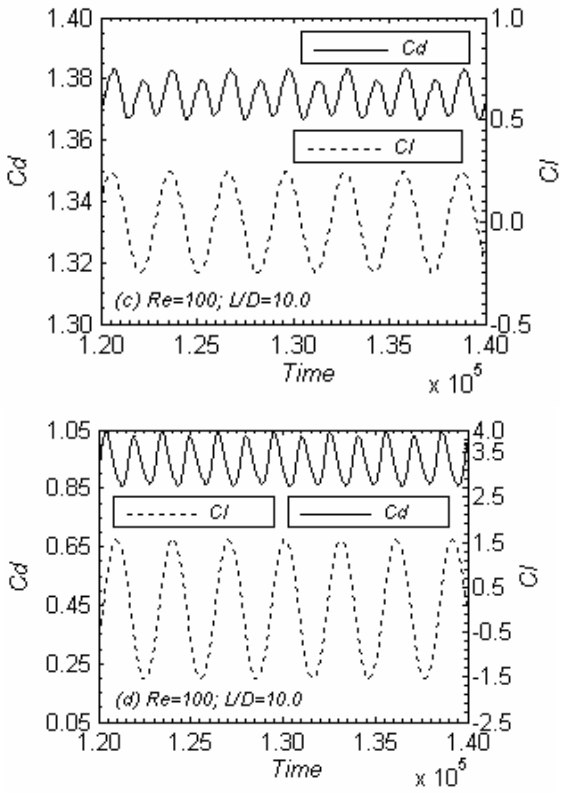

Fig. 5 Variation of lift and drag coefficient for spacing ratio 10.0. (a) *Cylinder1*, (b) *Cylinder2*, (c) *Cylinder3*, (d) *Cylinder4*

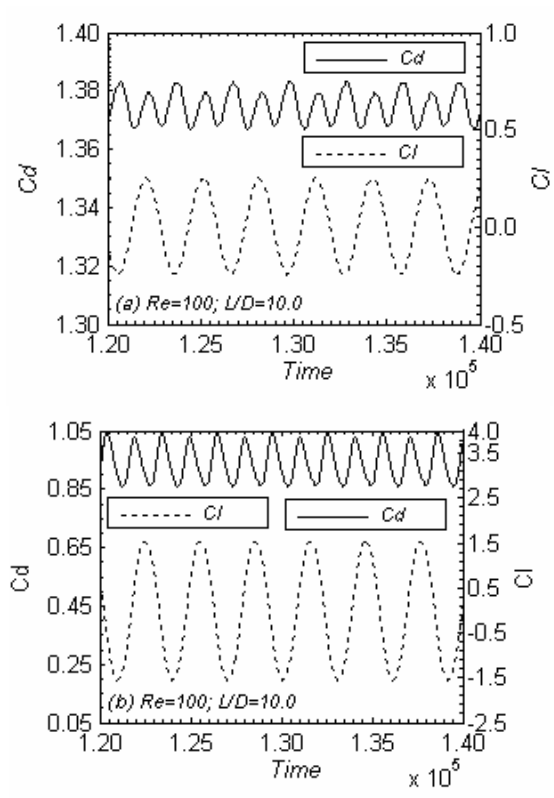

The mean value of drag coefficient, C_{dmean}, is presented in Fig. 6 as a function of L/D. Some experimental and numerical data published in the literature for single square cylinder are also given in the figure for comparison. It is shown that, as spacing ratio increases, the calculated mean drag coefficient initially decreases and then increases and finally almost constant for upstream and downstream cylinders. The calculated mean drag coefficient also shows that the computed results of cylinders 1 and 3 and those of cylinders 2 and 4 are almost equal (see Fig. (6)). Cylinders 2 and 4 are mostly located in the wake of cylinders 1 and 3. As a result, the free shear layers generated from outside of cylinders 1 and 3 reattaches onto cylinders 2 and 4, respectively, when the spacing ratio is small. The results further show that there is an abrupt increase in mean drag coefficient between spacing ratios 2.5 and 4 for cylinders 2 and 4. This is due to the flow pattern transformation. The changes in the flow pattern due to spacing ratio will be discussed later in subsequent section. It is also found that there is a significant difference for mean drag coefficients between cylinders 1, 3 and 2, 4 in the spacing ratio ranging from 0.5 to 2.5; this means that the flow experiences a significant flow pattern transformation in this region.

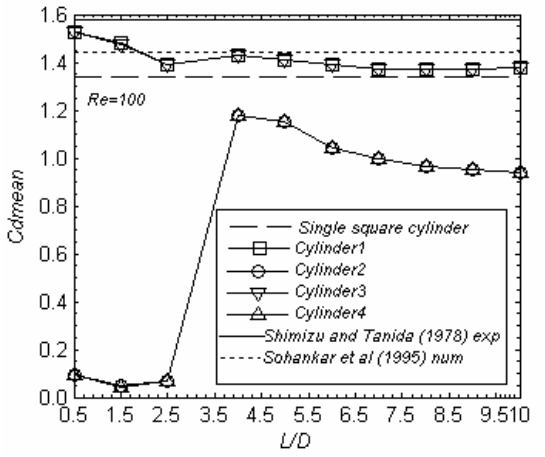

Fig. 6 Mean drag coefficient as a function of L/D for Reynolds number 100

The root-mean-square values of drag and lift coefficients, C_{drms} and C_{lrms}, are illustrated in Figs. 7 and 8, respectively. In general, the root-mean-square value of the drag coefficients of cylinders 1 and 3are almost equal, so are those of cylinders 2 and 4. The abrupt changes 1 and 3 and those of cylinders 2 and 4 for small spacing ratios 0.5, 1.5, 2.5 and 4.0 shows that the free shear layers generated from upstream cylinders 1 and 3 from inner and outer side reattaches onto cylinders 2 and 4. However, as spacing ratios increases from 4.0 to 10.0 the root-mean-square value of the drag coefficient decreases and increases for cylinders 2 and 4 for spacing ratios 9 and 10 and almost constant for cylinders 1 and 3 for spacing ratios 9 and 10. This suggests that the effects are caused by changes in the formation and shedding of the vortices with the increasing presence of spacing ratios (see Fig. 7).

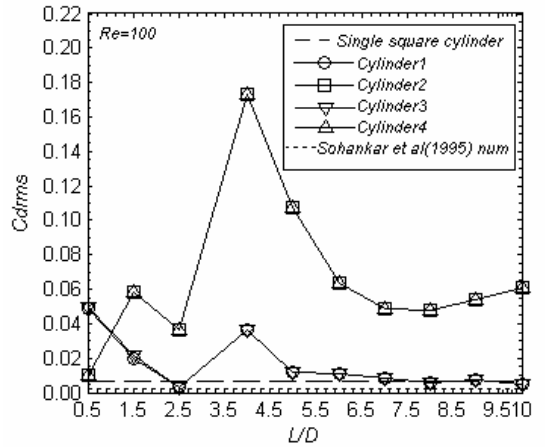

Fig. 7 Variations of the root-mean-square values of drag coefficient with the spacing ratio L/D.

At small spacing ratios, root-mean-square value of the lift coefficient is very low. When the upstream cylinders 1 and 3 starts to shed vortices, depending on the spacing ratios, root-mean-square values of the lift coefficient are increased either after spacing ratio 1.5 or 2.5. However at any particular spacing ratio, with increasing spacing ratio, root-mean-square value of the lift coefficient is observed to increase first and decrease later and for some cases almost constants. The root-mean-square values for the upstream cylinders 1 and 3 observed to be lower than that of downstream cylinders 2 and 4 for all chosen spacing ratios except that at spacing ratio 0.5 (see Fig. 8).

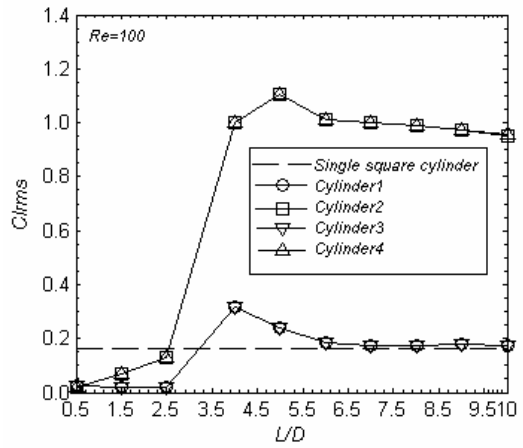

Fig. 8 Variations of the root-mean-square values of lift coefficient with the spacing ratio L/D

B. Vortex shedding frequency

Fourier spectrum analysis of the lift coefficients are carried out for two spacing ratios 1.5 and 10.0 to obtain the Strouhal number. It is to be noted that the Strouhal number is identified based on the dominating frequency in the corresponding spectra. The results for four cylinders are illustrated in Fig. 9 for spacing ratio 1.5 and in Fig. 10 for spacing ratio 10.0. Four graphs in Fig. 10 show a single dominant peak. This is related to the vortex shedding frequency. For small spacing ratios, there is definite peak in the spectra, which gives the predominant non-dimensional shedding frequency called the Strouhal number. Further, a vortex shedding from the upstream cylinders 1 and 3 hit the downstream cylinders 2 and 4 and at the same time the downstream cylinders develops its own vortices. As a result the upstream cylinders 1 and 3 and downstream cylinders 2 and 4 interact with each others and generate a complicated multi frequency with different values and strength in Fig. 9. For higher spacing ratios, both the upstream cylinders 1 and 3 and downstream cylinders 2 and 4 together behave like one cylinder and they get the same single dominant peak in the spectra (see Fig. 10).

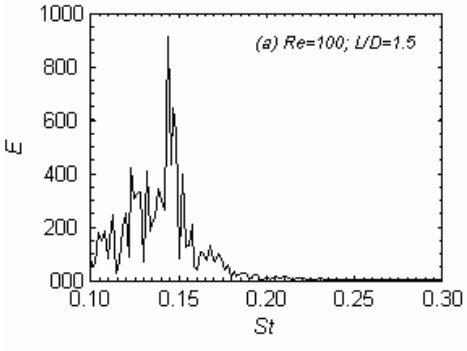

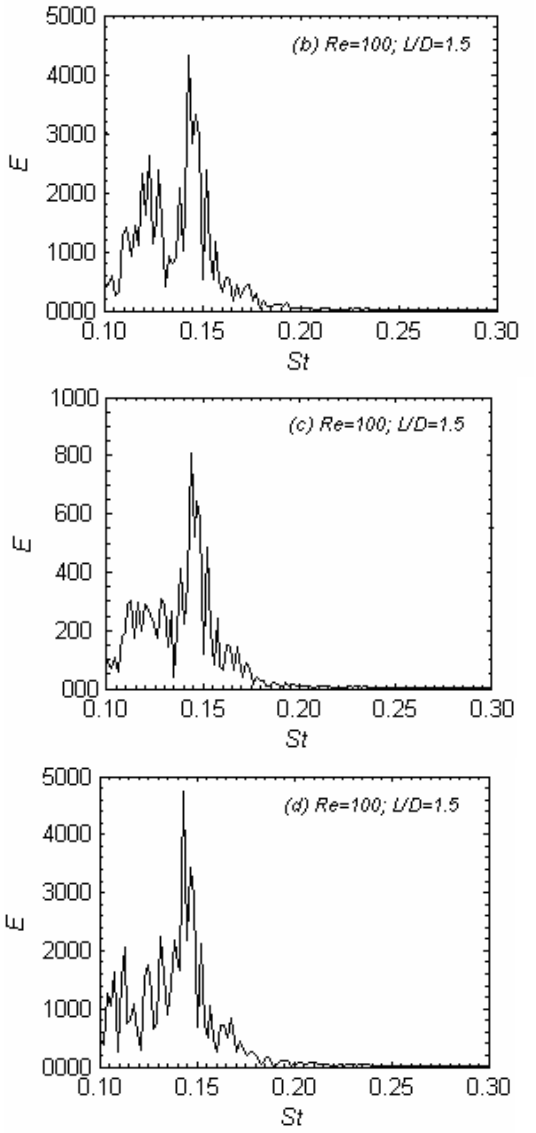

Fig. 9 Fourier spectrum analysis of lift coefficient for spacing ratio 1.5(a) Cylinder1, (b) *Cylinder2*, (c) *Cylinder3*, (d) *Cylinder4*

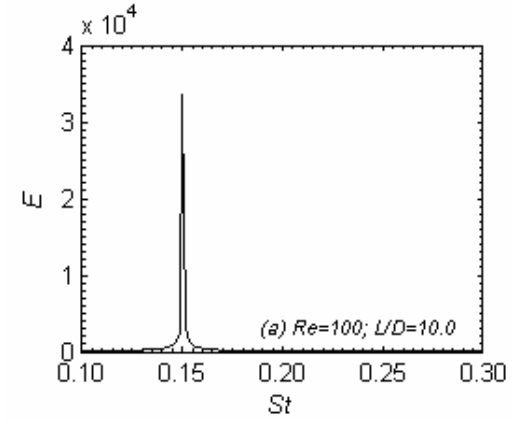

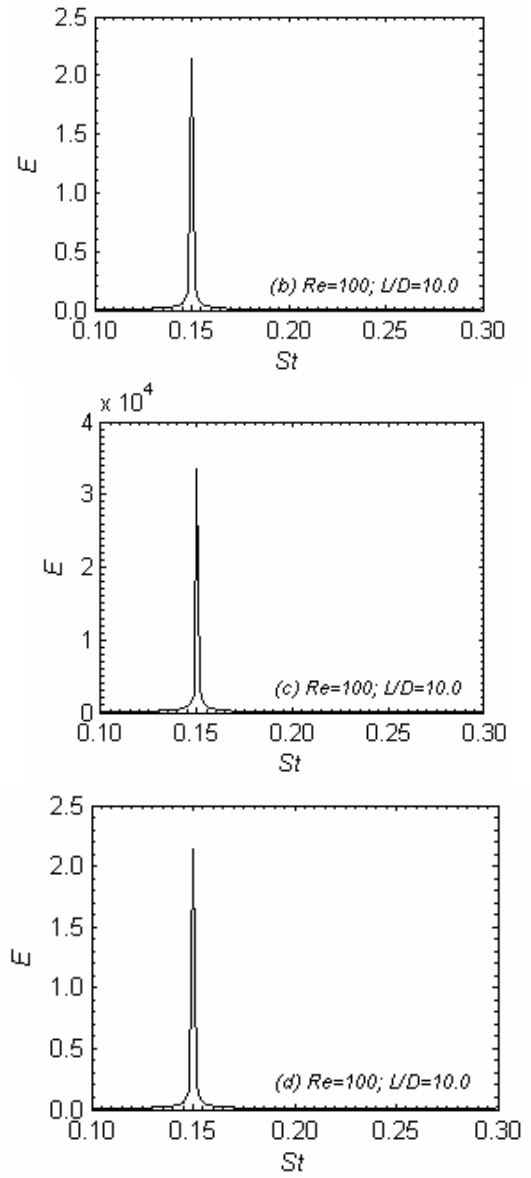

Fig. 10 Fourier spectrum analysis of lift coefficient for spacing ratio 10.0 (a) Cylinder1, (b) Cylinder2, (c) Cylinder3, (d) Cylinder4

More detailed variations of *St* with spacing ratios L/D for the chosen Reynolds number are summarized in Fig. 11. Some experimental and numerical data published in the literature for single square cylinder are also given in the figure for comparison. It is noteworthy in general, the Strouhal numbers of upstream cylinders 1 and 3 and those of downstream cylinders 2 and 4 are almost same for all chosen spacing ratios (see Fig. (11)). Figure 11 shows that Strouhal number decreases up to spacing ratio 2.5 and then increases up to spacing ratio 6.0. But for spacing ratio 7.0, the Strouhal number decreases a bit and then increases for remaining spacing ratios. The agreement between the experimentally measured Strouhal number and the computational results is quite reasonable for all four cylinders when the spacing ratios increase from 4.0 to 10.0. There exist some regions in which the Strouhal number for all four cylinders is much higher or

lower than that for the single square cylinder (see Fig. (11)). The results further show that the Strouhal number for all four cylinders is lower than that for the single square cylinder at the spacing ratio 2.5.

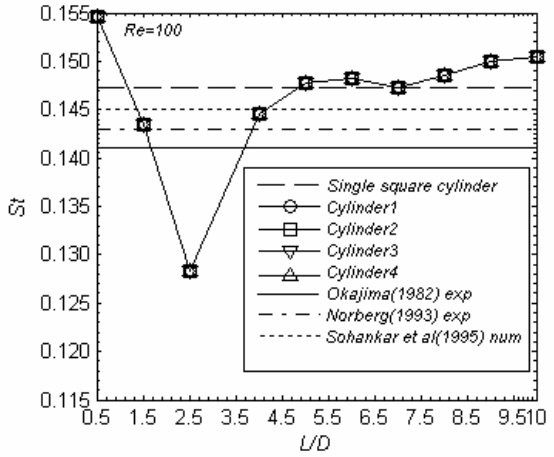

Fig. 11 Strouhal number as a function of the spacing ratio for four cylinders.

C. Flow structures in the wake

Vortex shedding is a comprehensive physical phenomenon. When it occurs, vortices are shed alternatively from the top and bottom of the cylinder. The shedding of vortices is always accompanied by some physical changes in the local flow and more complicated when there are upstream cylinders in the wake of downstream cylinders. The vorticity contours in the near wake of the cylinder are presented in Fig. 12. The negative vorticity (clockwise vortex) is shown by dashed lines and the positive one (anticlockwise vortex) by solid lines. For indication, instantaneous flow fields for a single square cylinder and for four cylinders near to each one are also presented in figs. 12(a) and (b), respectively. In the case of a single square cylinder, the necessary features of the vortex shedding mechanism are similar as those in the circular cylinder case, apart from the separation points of the boundary layers on the cylinder surface are fixed at the upstream corners of the square cylinder (see Fig. 12 (a)). The results further shows that when the cylinders are nearly closed to each one, they behave like a single square cylinder (see Fig. 12 (b)). Inoue [12] also observed such flow pattern for two side-by-side square cylinders. In Fig. 12 (c), two inner side free shear layers from the upstream cylinders reattach onto the two downstream cylinder surfaces. But, the outside free shear layers from upstream cylinders 1 and 3 do not reattach on the downstream cylinders 2 and 4 surfaces. As a result, the downstream cylinders are completely engulfed. It is also found from the study that both free shear layers from inner and outer side do not show any significant wiggling. This type of flow pattern is so called stable shielding flow pattern. One of the results from these investigations is shown in Fig. 12 (d) for $L/D = 2.5$. It is found that the two inner side free shear layers reattach to the downstream cylinder surface while the outer free shear layers do not reattach to the downstream cylinder surface. As a result the free shear layers from outer side alternately wiggling near the downstream cylinders. Such type of flow pattern is referred to as wiggling shielding flow pattern. In case of wiggling shielding flow pattern the Strouhal number is much less than that for the single square cylinder (see Fig. 11). The vortex shedding flow pattern has shown in Figs. 12 (e) and (f), respectively. This observation shows that the free shear layers on the upstream cylinder roll up into mature vortices and then impinge on the downstream cylinder. It is further found that when the spacing ratio is large enough the vortex shedding pattern occurs and as a result the alternate vortices from upstream cylinders are fully developed (see Fig. 12 (f)). The variation of the wake pattern with the spacing shown in Figs. 12(c-e) qualitatively quite similar to that observed for the four circular cylinders in an in-line square configuration numerically by Lam *et al* [11].

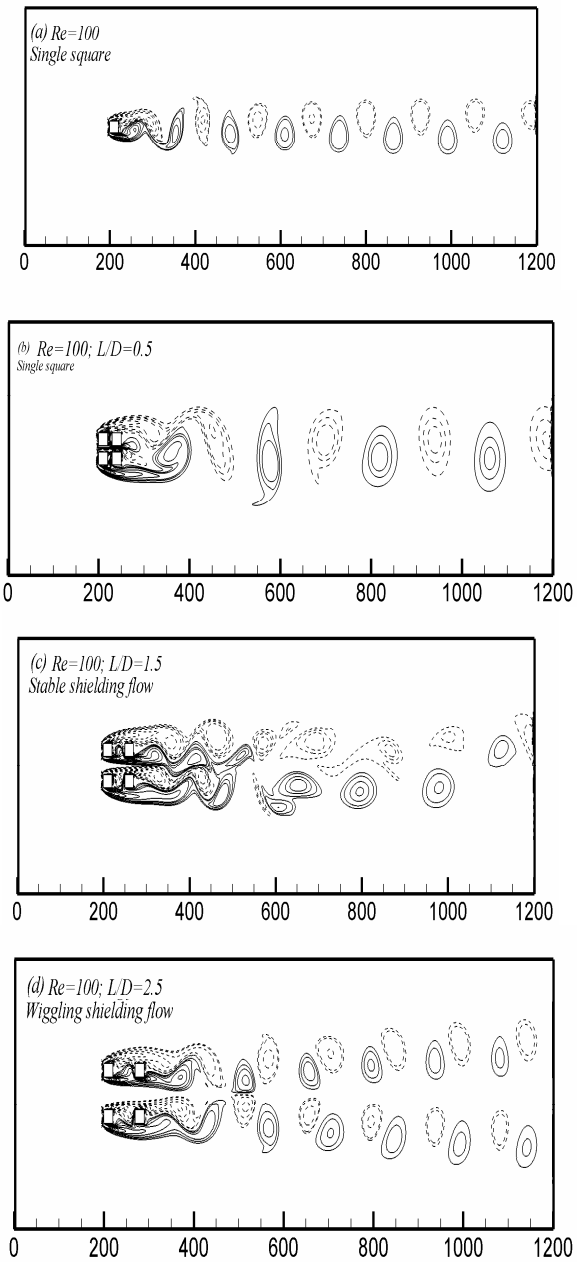

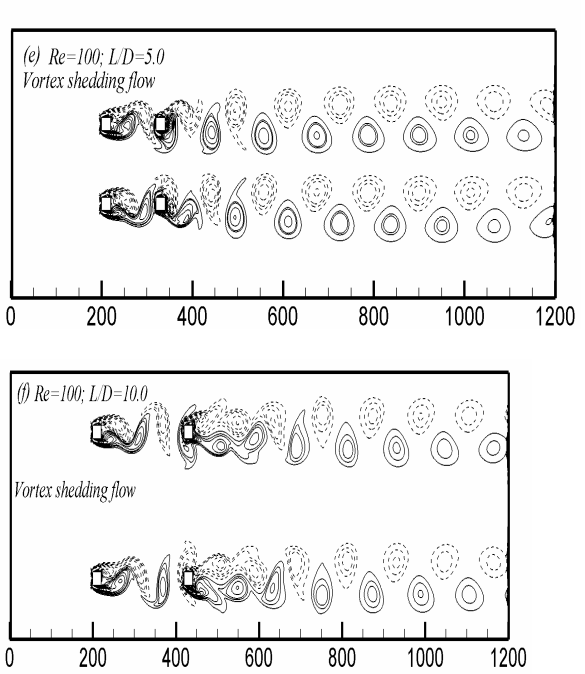

Fig. 12 Instantaneous vorticity contours for some spacing ratios: (a) Single square cylinder; (b) $L/D=0.5$; (c) $L/D=1.5$; (d) $L/D=2.5$; (e) $L/D=5.0$ and (f) $L/D=10.0$

V. Conclusion

This paper presents a numerical study of a uniform flow past four cylinders in an in-line rectangular configuration using the lattice Boltzmann method. The calculated results are compared with previous experimental and numerical results from single square cylinder and four cylinders in square configuration for circular cylinders. Four different flow patterns around the four cylinders are observed. At spacing ratio 0.5, only the single square cylinder flow pattern was observed. The stable shielding flow pattern was observed at spacing ratio 1.5, wiggling shielding flow pattern was observed at spacing ratio 2.5 and a vortex shedding flow pattern was observed at an even higher spacing ratio of 5.0. It is found that at small spacing ratios, there was more than one dominating frequency. It is also found that the Strouhal number for all four cylinders are almost equal for all chosen spacing ratios even there are more than one dominant frequency for small spacing ratios. It is found that there exist some regions in which the Strouhal number for all four cylinders is much higher at spacing ratio 0.5 and is much lower than at spacing ratio 2.5 compared to single square cylinder. A jump change in the physical quantities such as mean drag coefficient, root-mean-square values of the lift and drag coefficients and Strouhal number is the main reason for flow pattern transition was also observed. It is apparent that the vortex formation depends strongly on the spacing ratio between four cylinders in an array. The three dimensional numerical investigation for four square cylinders in an in-line rectangular configuration will be taken in near future.

Acknowledgment

The study described in this research was supported by a grant from National Science Foundation of China (Project No. 90715031). The financial support is gratefully acknowledged.

References

[1] M. M. Zdravkovich, "The effects of interference between circular cylinders in cross flow," Journal of Fluids and Structures, 1, 1987, pp. 235-261.
[2] A. T. Sayers, "Flow interference between four equispaced cylinders when subjected to a cross flow," Journal of Wind Engineering and Industrial Aerodynamics, 31, 1988, pp. 9-28.
[3] A. T. Sayers, "Vortex shedding from groups of three and four equispaced cylinders situated in cross flow," Journal of Wind Engineering and Industrial Aerodynamics, 34, 1990, pp. 213-221.
[4] K. Lam, and S. C. Lo, "A visualization study of cross-flow around four cylinders in a square configuration," Journal of Fluids and Structures, 6, 1992, pp. 109-131.
[5] K. Lam, and X. Fang, "The effect of interference of four equispaced cylinders in cross flow on pressure and force coefficients," Journal of Fluids and Structures, 9, 1995, pp. 195-214.
[6] M. M. Zdravkovich, "Flow around circular cylinders", 2003, Oxford University Press, Oxford.
[7] C. Norberg, "Fluctuating lift on a circular cylinder: review and new measurements", Journal of Fluids and Structures, 17, 2003, pp. 57-96.
[8] T. Farrant, M. Tan, and W. G. Price, "A cell boundary element method applied to laminar vortex shedding from array of cylinders in various arrangement", Journal of Fluids and Structures, 14, 2000, pp. 375-402.
[9] K. Lam, R. M. C. So, and J. Y. Li, "Flow around four cylinders in a square configuration using surface vorticity method", In: Proceedings of the Second International Conference on Vortex Methods, Istanbul, Turkey , 2001a.
[10] K. Lam, J. Y. Li, K. T. Chan, and R. M. C. So, "Velocity map and flow pattern of flow around four cylinders in a square configuration at low Reynolds number and large spacing ratio using particle image velocimetry", In:Proceddings of the Second International Conference on Vortex Methods, Istanbul, Turkey, 2001b.
[11] K. Lam, W. Q. Gong, and R. M. C. So, "Numerical simulation of cross-flow around four cylinders in an in-line square configuration", Journal of Fluids and Structures, 1, 2008, pp. 34-57.
[12] O. Inoue, W. Iwakami, and N. Hatakeyama, "Aeolian tones radiated from flow past two square cylinders in a side-by-side arrangement", Physics of Fluids, 18, 2006, pp. 1-18.
[13] Y. Rao, Y. S. Ni, and C. F. Liu, "Flow effect around two square cylinders arranged side by side using lattice Boltzmann method", International Journal of Modern Physics C, 19, 2008, pp. 1683-1694.
[14] T. Degawa, and T. Uchiyama, "Numerical simulation of bubbly flow around two tandem square section cylinders by vortex method", Journal of Mechanical Engineering Science, 222, 2008, pp. 225-234.
[15] Y. Shimizu, and Y. Tanida, "Fluid forces acting on cylinders of rectangular cross-section", Trans. JSME, 16, 1978, pp. 465-485.
[16] A. Okajima, "Strouhal numbers of rectangular cylinders", Journal of Fluid Mechanics, 123, 1982, pp. 379-398.
[17] C. Norberg, "Flow around rectangular cylinders: Pressure forces and wake frequencies", Journal of Wind Engineering and Industrial Aerodynamics, 49, 1993, pp. 187-196.
[18] A. Sohankar, L. Davidson, and C. Norberg, "Numerical simulation of unsteady flow around a square two-dimensional cylinder", The Twelfth Australian Fluid Mechanics Conference, The University of Sydney, Australia, 1995, pp. 517-520.
[19] S. U. Islam, and C. Y. Zhou, "Characteristics of flow past a square cylinder using the lattice Boltzmann method", to be published in Information Technology Journal.
[20] Z. Guo, B. Shi, and N. Wang, "Lattice BGK Model for Incompressible Navier-Stokes Equation", Journal of Computational Physics, 165, 2000, pp. 288-306.
[21] P. L. Bhatnagar, E. P. Gross, M. Krook, "A model for collision processes in gases. 1. small amplitude processes in charged and neutral one-component systems", Phys. Rev. 94, 1954, pp. 511-514.
[22] S. Chapman, T. Cowling, and D. Burnet, "The mathematical theory of non-uniform gases. An account of the kinetic theory of viscosity,

thermal conduction, and diffusion in gases", Cambridge University Press, 3rd edition, 1990.
[23] Y. Dazhi, M. Renwei, L. S. Luo, and S. Wei, "Viscous flow computations with the method of lattice Boltzmann equation", Progress in Aerospace Sciences 39, 2003, pp. 329-367.